Biophysical Chemistry 159 (2011) 267–274

Contents lists available at ScienceDirect

Biophysical Chemistry

journal homepage: http://www.elsevier.com/locate/biophyschem

Three-state thermal unfolding of onconase

Salvador Casares-Atienza [a], Ulrich Weininger [b], Ana Cámara-Artigas [c], Jochen Balbach [b], Maria M. Garcia-Mira [a,*]

[a] Departamento de Química Física, Facultad de Ciencias, Universidad de Granada. Avda. Fuentenueva s/n. 18071 Granada, Spain
[b] Institut für Physik, Biophysik, Martin-Luther-Universität Halle-Wittenberg, 06120 Halle (Saale), Germany
[c] Departamento de Química Física, Bioquímica y Química Inorgánica, Universidad de Almería, Carretera Sacramento s/n. 04120 Almería, Spain

HIGHLIGHTS

- In the 2.0–6.0 pH range, the thermal unfolding of onconase takes place via, at least, one equilibrium intermediate.
- This intermediate implies exposure of hydrophobic surface and changes around Trp3.
- 25% of the total enthalpy change upon unfolding takes place in the native to intermediate transition.
- The stability of the intermediate is close to that of the native state.

GRAPHICAL ABSTRACT

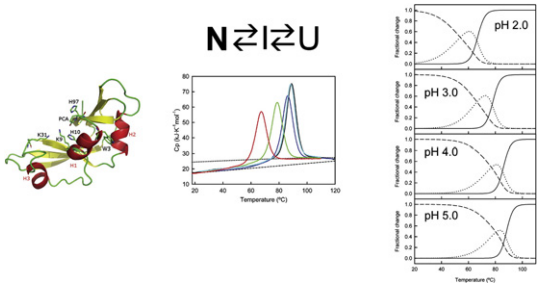

ARTICLE INFO

Article history:
Received 15 June 2011
Received in revised form 18 July 2011
Accepted 19 July 2011
Available online 24 July 2011

Keywords:
Onconase
Protein folding
Thermal unfolding
Folding equilibrium intermediate
Differential scanning calorimetry

ABSTRACT

Onconase is a member of the ribonuclease A superfamily currently in phase IIIb clinical trials as a treatment for malign mesothelioma due to its cytotoxic activity selective against tumor-cells. In this work, we have studied the equilibrium thermal unfolding of onconase using a combination of several structural and biophysical techniques. Our results indicate that at least one significantly populated intermediate, which implies the exposure of hydrophobic surface and significant changes in the environment around Trp3, occurs during the equilibrium unfolding process of this protein. The intermediate begins to populate at about 30° below the global unfolding temperature, reaching a maximum population of nearly 60%, 10° below the global unfolding temperature.

1. Introduction

Onconase is a ribonuclease originally obtained from *Rana pipiens* that belongs to the ribonuclease A superfamily. It displays a high *in vivo* cytotoxic activity, and this activity is selective against tumor-cells [1–3]. For this reason, it is currently in advanced phase IIIb clinical trials as a treatment for malign mesothelioma [4,5]. Moreover, onconase has also been shown to possess antiviral activity, i.e. inhibits the replication of HIV-1 in chronically infected human cells [6–8]. During clinical trials, the main side effect associated to its delivery was reversible renal toxicity [9,10], which is probably caused by the unusually high stability of onconase [11].

It is broadly believed that single domain proteins have evolved in order to disfavor the population of intermediate states [12]. However, partially folded states, or folding intermediates, may be of biological relevance. As an example, we can consider the case of the structural proteins actin as well as alpha and beta tubulins, which fold via intermediates exposing a high proportion of hydrophobic surface. These

Abbreviations: CD, circular dichroism; NMR, nuclear magnetic resonance; DSC, differential scanning calorimetry; ANS, 8-anilino-1-naphtalenesulfonate; RCSB, Research Collaboratory for Protein Bioinformatics; PDB, Protein Data Bank; ESRF, European Synchrotron Radiation Facility; rmsd, root mean square deviation; ECP, eosinophil cationic protein; BMRB, Biological Magnetic Resonance Bank.

* Corresponding author. Tel.: +34 958241000 20283; fax: +34 958272879.
E-mail address: mdmar@ugr.es (M.M. Garcia-Mira).

0301-4622/$ – see front matter © 2011 Elsevier B.V. All rights reserved.
doi:10.1016/j.bpc.2011.07.005

intermediates constitute the building blocks co-assembling into the long polymeric structures present in the cytoskeleton [13]. Nevertheless, intermediates are normally observed as something undesirable, since their presence may be related with irreversible processes such as protein aggregation or amyloid formation [14–16]. On the other hand, when designing the activity or stability of a protein, it is very important to consider the intermediate species, because they define the "operative" stability of the protein [17]. Usually, the intermediate lacks protein activity, and thus, the transition between the native-state and the intermediate is the one that is biologically relevant, even if it is observed as a smaller transition in the stability profile of the protein. Therefore, for proteins of industrial or pharmaceutical interest, as onconase, it is very important to gain a deep knowledge of their unfolding mechanisms. In onconase's case, this knowledge is even more important, since the side effects associated to its delivery to patients might be related with the global stability of the protein [10]. In other words, if onconase has an intermediate, its beneficial activity could be lost in the transition from the native protein to the intermediate, but the harmful effects would not disappear until the protein totally unfolds.

To distinguish two-state from other types of equilibria, it is well established that a good strategy is to investigate protein folding using several techniques, probing different structural features [18–21]. In this work we have studied the thermal unfolding of onconase using a broad range of different techniques: circular dichroism (CD), intrinsic fluorescence, nuclear magnetic resonance (NMR), differential scanning calorimetry (DSC) and 8-anilino-1-naphtalenesulfonate (ANS) binding. We have found that onconase seems to unfold via one significantly populated equilibrium intermediate, which implies the exposure of hydrophobic surface and significant changes in the environment around Trp3 and whose stability is close to that of the native protein.

2. Materials and methods

2.1. Materials

The pET-22b(+) plasmid carrying the sequence of onconase was a kind gift of Alfacell Corp. (Somerset, NJ, USA). Vector pET-26b(+) was purchased from Novagen (Madison, WI, USA). Cell strains were acquired from Stratagene (La Jolla, CA, USA) and growth media from Difco (Kansas City, MO, USA). All other chemicals were bought from Sigma-Aldrich (St. Louis, MO, USA).

2.2. Protein expression, purification and sample preparation

Wild-type onconase was cloned into pET-26b(+) by Top Gene Technologies (Montreal, Canada). Onconase was grown in terrific broth, overexpressed overnight in *Escherichia coli* BL21(DE3), purified as previously described [22] and later shock frozen, stored at −80 °C and/or lyophilized. The purity and molecular weight of the samples were checked by mass spectroscopy. The correct folding of the protein was verified by native electrophoresis and by means of x-ray diffraction. Besides, the crystallographic structure shows the presence of the pyroglutamic acid at the N-terminal of our samples. Buffers showing low protonation enthalpies as well as low dependence of their pKa-values with temperature were chosen to carry out the experiments. Thus, glycine/HCl 20 mM buffer was used for pH 2.0 and 3.0, and sodium acetate 20 mM for pH 4.0 and 5.0. Experiments at pH 6.0 and 7.0 were performed in, both, sodium cacodylate 20 mM, as well as in sodium phosphate 20 mM, to rule out stabilization of onconase by phosphate anions. Samples for DSC were prepared by exhaustive dialysis for at least 24 hours against the working buffer. For the other techniques, samples were prepared passing the protein through a PD MidiTrap column (GE Healthcare, Chalfont St. Giles, UK). The concentration of the protein was determined using an absorption coefficient [11] of 10,400 M^{-1} cm^{-1} at 280 nm.

2.3. Crystallization and data collection

The purified recombinant onconase was concentrated to approximately 10 mg·mL^{-1} using a Microcon YM-3 (Millipore, Billerica, MA, USA). Crystals were grown using the counter-diffusion technique as described in Camara-Artigas et al. [23]. The best crystals were obtained in 4 M Ammonium sulphate and 0.1 M sodium acetate at pH 4. For data collection, crystals were soaked in 20% glycerol inside the capillary and placed in a cold nitrogen stream maintained at 110 K. X-ray diffraction data collection was performed at the beamline BM-16 station of the European Synchrotron Radiation Facility (ESRF) using a 0.97 Å wavelength in a Mar CCD-165 detector. Data were indexed, integrated and scaled with the HKL2000 suite [24]. The crystallographic parameters and statistics of the data collection are listed in Table 1.

2.4. Structure resolution and refinement

Initial phasing was performed using Molrep [25]. The Matthews coefficient [26] was 1.97 with a solvent content of 37.63% for one molecule at the asymmetric unit. The coordinates of natural onconase, without ligand and water molecules, were used as a search model (PDB code 1onc). A clear peak was obtained with an initial R factor of 43.7%. Initial refinement using 10 cycles of restrained positional refinement with the program REFMAC5 quickly dropped the R factor to 26.86%. Manual building was performed using the resulting σA-weighted (2Fo − Fc) and (Fo − Fc) electron density maps and the program COOT [27]. In addition to water molecules, several solvent molecules were clearly identified in the electron density difference maps: four sulfate ions and one glycerol. Structure superposition and rmsd calculations were performed using the CCP4 modules LSQKAB and TOP [28]. Before deposition, the quality of the structure was checked using the MolProbity web server [29] and PROCHECK [30]. Refinement statistics are collected in Table 1. The coordinates and structure factors were deposited at the RCSB PDB with entry code 3hg6.

2.5. Circular dichroism and fluorescence experiments

Thermal unfolding transitions of onconase were monitored by CD at 291 nm using a JASCO J600A spectropolarimeter (Jasco Inc.) equipped

Table 1
X-ray data collection and refinement statistics.

	Onconase WT
Space group	$P2_12_12_1$
Unit cell dimensions a b c	32.516 39.799 68.536 90.000 90.000 90.000
Resolution range (Å)	20–1.7
Number of observations	543678
Unique reflections	9807 (838)
Data completeness (%)	95.5 (83.6)
R_{merge}[a] (%)	12.8 (49.8)
I/σ(I)	15.4 (3.8)
Refinement	
Protein residues	104
Solvent	97
R_{work} (%)	18.7 (30.8)
R_{free} (%)	24.39 (42.5)
rms deviations from ideal geometry	
Bonds (Å)	0.020
Angles (degrees)	2.165
Mean B (protein) (Å^2)	15.08
Residues in allowed regions of the Ramachandran plot (%)[b]	100

The values in parentheses are for the highest resolution bin.
[a] $Rsym = \Sigma_h\Sigma_l|I_{hl} - \langle I_h\rangle|/\Sigma_h\Sigma_l\langle I_h\rangle$, where I_l is the lth observation of reflection **h** and $\langle I_h\rangle$ is the weighted average intensity for all observations l of reflection **h**.
[b] From program PROCHECK statistics.

with a peltier element and by fluorescence emission at 330 nm using a Cary Eclipse spectrofluorimeter (Varian Inc.) exciting the samples at 298 nm. Protein concentration ranged from 1.5 to 75.0 μM in Gly/HCl 20 mM (pH 2.0). The thermal dependence of ANS (8-anilino-1-naphtalenesulfonate) binding to onconase was also studied using a Cary Eclipse spectrofluorimeter at 480 nm after excitation at 370 nm. Protein and ANS concentrations were 5 and 250 μM respectively, as in previous studies with onconase [31], at pH 2.0.

Measurements were taken introducing a temperature probe in the measuring cuvette (CD) during the experiment, or, alternatively, the spectrometer was calibrated the same day the experiments were carried out using an external temperature probe, the same cuvette and the same buffer volume as throughout the experiment with onconase (intrinsic fluorescence and ANS binding experiments). All experiments were carried out at a heating rate of 1 K min^{-1}.

The transitions were analyzed on the basis of the two-state model using SigmaPlot (SPSS Inc.) as previously described [32] with a fixed heat capacity change value of 5 kJ mol^{-1} K^{-1}, the expected value for a protein with the amino acidic composition of onconase [33,34].

2.6. Fluorescence quenching experiments

Acrylamide and cesium chloride intrinsic fluorescence quenching of the only tryptophan residue of onconase, Trp3, was monitored by the loss of fluorescence emission at 330 nm using a Cary Eclipse spectrofluorimeter (Varian Inc.) exciting the samples at 298 nm. Intrinsic fluorescence emission spectra were recorded from 310 to 450 nm using a 1 cm path length cuvette at 25 °C and 60 °C, using 10 nm for both excitation and emission slits. Experiments were carried out in Gly/HCl 20 mM, pH 2.0. Protein concentration of the samples was 5 μM and quencher concentration ranged from 0 to 1 M. Samples were incubated for 15 min at the desired temperature to ensure proper equilibration.

2.7. Nuclear magnetic resonance

^{1}H-1D spectra were acquired on a Bruker Avance II 600 spectrometer. The sample contained 500 μM onconase in Gly/HCl 20 mM, D_2O 10%, pH 2.0. The spectra were recorded between 30 and 80 °C in steps of two degrees. Prior to data acquisition, the probe was allowed to equilibrate for 5 min after the desired temperature was reached. Temperature was calibrated using a sample of 100% ethylene glycol the same day the thermal transition was measured. All spectra were processed and analyzed using Felix 2000. Since the intensity of exchangeable protons (amide tryptophan indol) is affected by faster exchange with the solvent at higher temperatures, these probes could not be used. Therefore, we focused on non-exchangeable protons of two upfield shifted methyl groups of the native state that do not interfere with signals from the unfolded state as well as the signals corresponding to methyl groups in the unfolded state.

2.8. Differential scanning calorimetry experiments

DSC experiments were carried out with a VP-DSC or a VP-Capillary DSC microcalorimeter from MicroCal (Northampton, MA). Experiments were performed at a scan rate of 0.5 K min^{-1} or 1.5 K min^{-1}. Protein concentration was kept between 0.3 and 1.2 mg mL^{-1}. The buffer of the last dialysis step was used for baselines and to fill the reference cell of the calorimeter. Several buffer-buffer baselines were completed to establish the proper equilibration of the calorimeter. In all cases, a reheating run was done to check the reversibility of the process. The transitions were analyzed on the basis of the two-state and the three-state models using SigmaPlot (SPSS Inc.). The two-state analysis was carried out as previously described [35]. For the three-state analysis we used the model we have previously described [18] with little modifications. In brief, our three-state model considers the heat capacity of the intermediate to be a linear combination of the heat capacity of both, native and unfolded states:

$$C_p(I) = (1-F)\cdot C_p(N) + F\cdot C_p(U) \quad (1)$$

where F is a parameter that can take values between 0 and 1. When F = 0, the heat capacity of the intermediate is equal to the heat capacity of the native protein and when F = 1, the heat capacity of the intermediate is equal to the heat capacity of the unfolded state. The value of F was kept fixed in each fitting, and then the fittings were repeated changing the value of F. The fits were found to be excellent for F values between 0 and 0.4.

To reduce the number of floating parameters during the fittings, we have considered for, both, the two-state as well as the three-state model that the unfolded baseline could be fitted to a quadratic equation [36] whose curvature was fixed to the expected values given by the Privalov and Makhatadze's set of parameters [34]. The two-state analysis was carried out twice: letting the slope of the dependence of the native heat capacity with temperature float and fixing it to the calculated value according to data in the literature [33]. For the three-state analysis the slope of the native baseline was always fixed to the value calculated for native onconase [33]. Errors in the different thermodynamic variables have been calculated as three times the fitting standard error or by propagation of errors [37,38].

3. Results and discussion

3.1. Structure of recombinant wild-type onconase by x-ray crystallography

Prior to the thermodynamic study of onconase, protein purity and integrity has been checked by SDS-page, native electrophoresis and mass spectroscopy: wild-type onconase monomers were the only species present in the samples. We have also crystallized and solved the structure of our recombinant onconase by x-ray crystallography (RCSB PDB with entry code 3hg6, Fig. S1, panel A, see Supplementary Material). Onconase shows a kidney-shaped fold with its active site located at the cleft between the two lobes. The N-terminal α-helix makes contact with both lobes and contains three residues implicated in the catalytic activity of onconase: the N-terminal pyroglutamic acid (Pca1), Lys9 and His10. The hydrogen bond between Pca1 and Lys9 stabilizes the rate-limiting transition state during catalysis [3]. We have compared our structure with the structure of onconase directly purified from *Rana pipiens* oocytes (PDB entry 1onc) and found no remarkable differences between them (Fig. 1). Both proteins crystallize in the same space group with nearly the same cell parameters. The pyroglutamate group present in the active site of natural onconase, that generates spontaneously upon cyclization of Gln1, can be easily identified in the electron difference maps of our

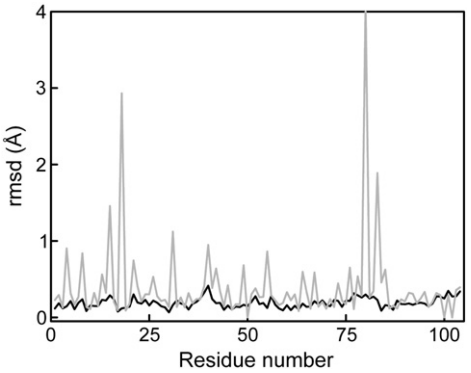

Fig. 1. Root mean square deviation (rmsd) representation of the difference in backbone (black) and side chains (gray) between the recombinant onconase (PDB code 3hg6) and the protein purified from *Rana pipiens* (PDB code 1onc).

recombinant protein as well (Fig. S1, panel B, Supplementary Material) The backbone structures of both, natural and recombinant proteins, are basically identical, as indicated by a rms deviation of only 0.191 when the backbone atoms are compared. Moreover, most of the side-chains also display the same orientation (Fig. 1) and the only significant differences are found in residues placed on the surface of the protein that participate in crystal contacts. Therefore, the unfolding behaviour of recombinant onconase cannot be attributed to the bacterial expression.

3.2. Equilibrium thermal denaturation experiments with onconase, in the 2.0–6.0 pH range cannot be interpreted using the two-state model

To study the unfolding mechanism of onconase, we have carried out the so-called superposition test [20] using several spectroscopic techniques and differential scanning calorimetry. Since each one of the techniques follows different physical properties and, therefore, structural probes, if a protein unfolds via a two-state mechanism, the model should fit well to all traces and, at the same time, the dependences of the native/unfolded protein population with temperature should superimpose for all techniques.

The main handicap to use spectroscopic techniques to study the thermal unfolding of onconase is its unusual stability. Around the physiological pH value, onconase is too stable and it is not possible to obtain complete transitions with unfolded baseline by spectroscopy. However, the shape of the temperature scans measured using differential scanning calorimetry (DSC) is very similar in the whole pH range we have studied (see Fig. 2). There are no apparent differences in the folding mechanism between acidic and neutral pH values. Thus, we have decided to carry out the spectroscopic measurements at pH 2.0, where the protein is destabilized and the transitions can be better evaluated.

We have compared the thermal unfolding of onconase measuring circular dichroism (CD) in the near-UV region (291 nm), tryptophan intrinsic fluorescence and nuclear magnetic resonance chemical shift perturbations in ^{1}H-1D spectra. Out of the full collection of signals of the protein displayed in the NMR spectra, only 3 sets could be clearly followed through the entire transition with a reasonable signal to noise ratio and without solvent exchange or overlapping problems. Two of them correspond to protons of upfield-shifted methyl groups of the native protein and the other one corresponds to protons of a methyl group of the unfolded state of the protein (methyl groups are virtually non-exchangeable). Based on the assignment of onconase C87A/C104A [39] (BMRB entry 16040), these methyl groups belong to Val17 and Ile37, which are localized in the hydrophobic core of the protein. Their upfield proton shift is caused by neighbouring phenylalanines. Unfortunately, the isolated signal belonging to the indol proton of Trp3, could not be used for this analysis since it converges to overlap with the signal corresponding to Asn92 amide proton as the temperature increases.

The two-state model could be very well fitted to the near UV-CD, intrinsic fluorescence and the three different sets of NMR signals that have been studied. But, even if the two-state model would fit very nicely to each one of the individual experimental transitions obtained using all three spectroscopic methods, once we plotted the results for the different techniques together (Fig. 3), it became clear that near-UV CD and fluorescence curves are superimposable, but are shifted about 7° below the curves corresponding to the NMR data. Such behaviour is incompatible with a two-state unfolding mechanism.

We have also studied the thermal unfolding of wild-type onconase at several pH-values, between 2.0 and 7.0, using DSC (Fig. 2). The transitions were reversible from pH 2.0 to pH 6.0. Above pH 6.0, the unfolding of onconase was found to be irreversible, even if the scans were stopped immediately after the transition peak. As expected, onconase resulted to be very stable, increasing its stability as pH increases. In the 5–6 pH range, the maximum of the DSC transition appears over 90 °C (Fig. 2).

The absolute heat capacity of unfolded onconase does not depend on the pH and agrees with the predicted values, as calculated using the Privalov and Makhatadze's set of parameters [34] for a protein with the sequence of onconase, in all the measured temperature range. However, the absolute heat capacity of the native state agrees with the predicted values for a globular protein of onconase's size [33] only at low temperatures. As temperature rises, a systematic increase of the native heat capacity (relative to the predicted values) is found at all the studied pH values (see Fig. 2).

The analysis of the DSC traces using the two-state model results in fittings that, at the first sight, can be acceptable (Fig. 4, upper panel). The ratio between the calorimetric and the van't Hoff enthalpy is close to 1, something that is usually interpreted as a marker of the goodness of the two-state model. The Tm calculated using this model coincides with the Tm values obtained from the analysis of the NMR data (see Fig. 3).

Nevertheless, in the pH range where the unfolding of onconase is reversible (2.0–6.0), the fitting of the two-state model to the experimental data resulted, in all cases, in systematic small deviations at the beginning of the transition. As a consequence, the obtained heat capacity functions for the native and unfolded protein cross at too low temperatures causing the calculated heat capacity changes upon unfolding to be negative. This fact would mean that, as onconase unfolds, there is an exposure of predominantly polar surface instead of apolar surface, something unrealistic for a soluble globular protein.

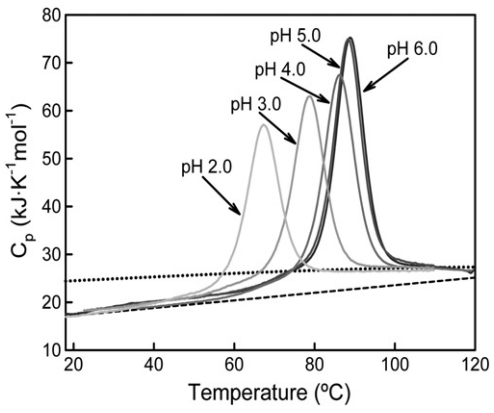

Fig. 2. DSC profiles of onconase in the pH 2.0–6.0 range. Experimental data (continuous lines), absolute heat capacity predicted for native onconase [33] (black dashed line) and predicted heat capacity values for unfolded onconase calculated using Privalov and Makhatadze's set of parameters [34] (black dotted line).

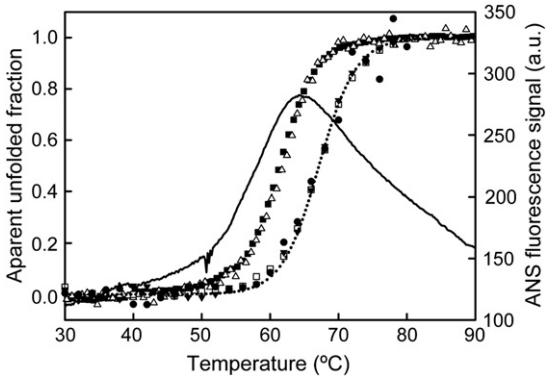

Fig. 3. Superposition test for onconase. Thermal unfolding at pH 2.0 monitored by near-UV CD (open triangles), emission fluorescence (closed squares), NMR (closed triangles: 0.56–0.63 ppm, closed circles: 0.64–0.89 ppm and open squares: −0.03 to 0.10 ppm) and DSC (dotted line). Data are shown as apparent unfolded fractions. On the right axis of the plot, the fluorescence of ANS in the presence of onconase is represented (continuous line).

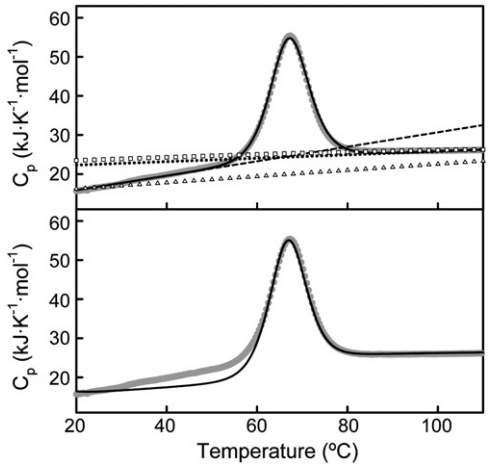

Fig. 4. Two-state analysis of DSC profiles of onconase 1.06 mg·mL^{-1} in Gly 20 mM, pH 2.0. Upper panel: experimental data (grey full circles), best fit of the two-state model letting the baselines float (continuous line), heat capacity of the native state calculated from the best fit of two-state model (dashed line), heat capacity of the unfolded state calculated from the best fit of the two-state model (open squares), absolute heat capacity predicted for native onconase [33] (open triangles) and predicted heat capacity values for unfolded onconase calculated using Privalov and Makhatadze's set of parameters [34] (dotted line). Lower panel: continuous line is the best fit of the two-state model fixing the baselines to the predicted values for native [33] and unfolded [34] onconase.

As an illustration, in the upper panel of Fig. 4, the absolute heat capacity, the predicted baselines for onconase, the two-state fitting and the baselines resulting from the two-state fitting to the thermal denaturation of the wild-type protein at pH 2.0 are represented. The slope of the native baseline given by the two-state fitting is too high and the baselines cross at 65 °C, very far away from the 140 °C at which calculations say this should happen [40]. When we repeated the fittings fixing the native and unfolded baseline to the expected values they should have according to Freire [33] and to the Privalov and Makhatadze's [34] set of parameters, we found, at all pH values, very clear deviations at the beginning of the peak that are usually considered to be indications of the non validity of the two-state model [41] (Fig. 4, lower panel).

To discard that the observed deviations from the two-sate behaviour could be due to kinetically controlled processes, DSC experiments at different scan rates (0.5 and 1.5 K·min^{-1}, data not shown) were carried out. In all cases, the traces at lower and higher scan rates are superimposable. Therefore, our DSC experiments are only showing processes occurring in equilibrium. In a similar way, oligomerization equilibria were discarded as the reason for the non-two-sate behaviour since no dependence of the transitions with the protein concentration was found in the circular dichroism or differential scanning calorimetry experiments (data not shown).

3.3. Equilibrium thermal denaturation experiments with onconase, in the 2.0–6.0 pH range, indicate the existence of a thermal equilibrium intermediate

Using, both, far-UV CD and tryptophan intrinsic fluorescence, we can follow the dependence with temperature of the changes in the environment around the only tryptophan of onconase (Trp3). Since the Tm values obtained from the analysis of far-UV CD and tryptophan fluorescence are lower than those obtained for DSC and NMR, this may indicate that onconase unfolds via at least one intermediate, as there seem to be changes around Trp3 happening before the global unfolding of the protein takes place.

We have studied, as well, the thermal dependence of ANS (8-anilino-1-naphtalenesulfonate) binding to onconase at pH 2.0. We found that the thermal dependence of ANS emission fluorescence in the presence of onconase displays a maximum at 63 °C (Fig. 3). A peak in ANS fluorescence in the presence of a protein is generally interpreted as a confirmation of the existence of an intermediate [42], since ANS fluorescence dramatically increases in a hydrophobic environment and, therefore, as it binds to hydrophobic patches. Thus, it is usually considered that binding of ANS should be stronger to molten globule-like intermediates than to the native and unfolded states of a protein. Therefore, the fact that ANS binds to onconase during unfolding suggests that the protein does unfold via an intermediate, and that the intermediate formation implies the exposure of some hydrophobic patches.

This result is also supported by intrinsic fluorescence quenching of Trp3 experiments at pH 2.0. Intrinsic fluorescence quenching of tryptophan residues has been extensively used to study protein folding intermediates in equilibrium [43,44] as well as in kinetic studies[43,45,46]. Using this technique, we have compared the solvent accessibility of Trp3 at 25 °C, where we expect the protein to be native, and 60 °C, in the region where the ANS binding experiments show a maximum. We have used two different quenchers: acrylamide (non polar) and Cs^+ (polar). We have found that Cs^+ does not promote fluorescence quenching at either of the two temperatures whereas the presence of acrylamide clearly reduces the intensity of Trp3 fluorescence at both temperatures (see Supplementary Material, Fig. S2). This result indicates that Trp3 is not solvent exposed, and the protein is not unfolded, at either temperature as only a non-polar quencher like acrylamide can

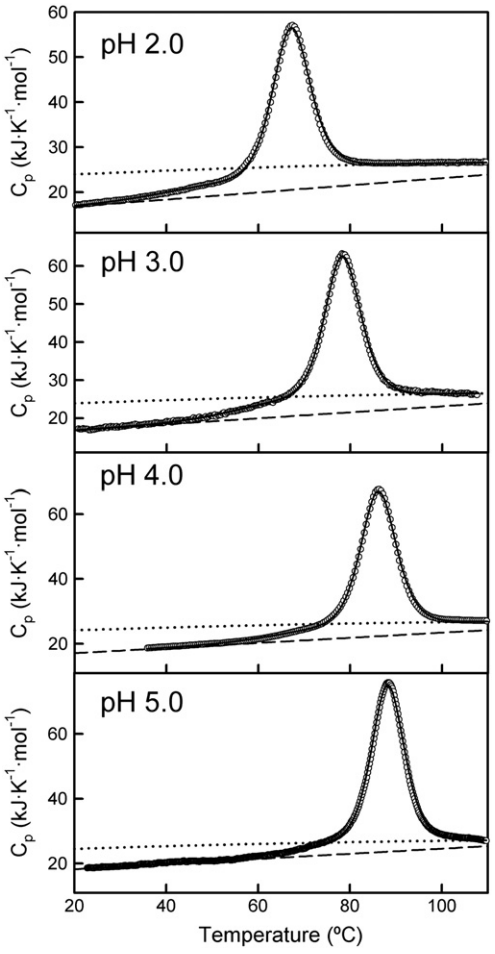

Fig. 5. Three-state analysis of DSC traces of onconase at different pH values. Experimental data (open circles), best fit of the three-state sequential model, considering a native-like heat capacity for the intermediate (continuous lines), heat capacity of the native and unfolded states of onconase resulting from the best fit of the three-state model (dashed and dotted lines).

interact with it. On the other hand, the quenching induced by acrylamide is dramatically enhanced when the protein samples are incubated at 60 °C compared with 25 °C, as indicated by the remarkable increase in the slope of the fluorescence intensity ratios, which is indicative of a higher accessibility of the region surrounding Trp3. This suggests that, at 60 °C, another species, different from the native or the unfolded states, should be populated. The region around Trp3 in this species should be, at least, partially loosen.

Based on all these evidence, we decided to use the three-state sequential model [17,18] to analyze our DSC experiments. Contrary to the two-state model, the fitting of the three-state model could reproduce very accurately the experimental data at all pH values (Fig. 5), and the resulting thermodynamic parameters, including heat capacity changes upon unfolding, are reasonable (Table 2). This model predicts the existence of a significantly populated equilibrium folding intermediate for onconase. For example, at pH 2.0, up to 60% of the molecules appear to be in the intermediate state at 61 °C (Fig. 6). Moreover, the temperature at which we expect the intermediate population to be maximal according to the DSC analysis is in very reasonable agreement with the maximum found in the ANS experiments (63 °C). Therefore, these data also indicate that there is an intermediate in the unfolding of onconase.

This possible intermediate even seems to be the most populated species within a narrow temperature range just before the transition to the unfolded state (Fig. 6). Our analysis does not find a strong dependence of the maximum intermediate population with the pH. The best fits are obtained when parameter F (the parameter measuring the similitude of the intermediate's heat capacity with those of native and unfolded state, see materials and methods) has values in the 0–0.4 range. This indicates that the heat capacity of the intermediate is more similar to the heat capacity of the native state than to the heat capacity of the unfolded state. The three-state sequential model also predicts the transition from the native to the intermediate state to involve about 25% of the total enthalpy change upon unfolding (Table 2). That means that the intermediate formation must imply the loss or weakening of some interactions in the protein.

Our results also point out that the intermediate formation during thermal-induced unfolding transitions is accompanied by some local unfolding and exposure of additional hydrophobicity in part of the protein, sensed by Trp3 (near UV-CD, intrinsic fluorescence and fluorescence quenching), ANS binding and a slight increase in the heat capacity compared to the native state, but without major changes in the overall tertiary structure of the rest of protein according to the NMR resonances (Val17 and Ile37), which could be analyzed so far.

This behaviour of onconase is very similar, for example, to the one of apoflavodoxin from *anabaena* [18,47]. Apoflavodoxin unfolds via an intermediate in which a considerable part of the protein remains close to the native fold and a 40 residue region is unfolded. In the case of apoflavodoxin, the intermediate only becomes apparent by the superposition test and by the cross of the baselines of DSC at low temperature, as it is the case of onconase.

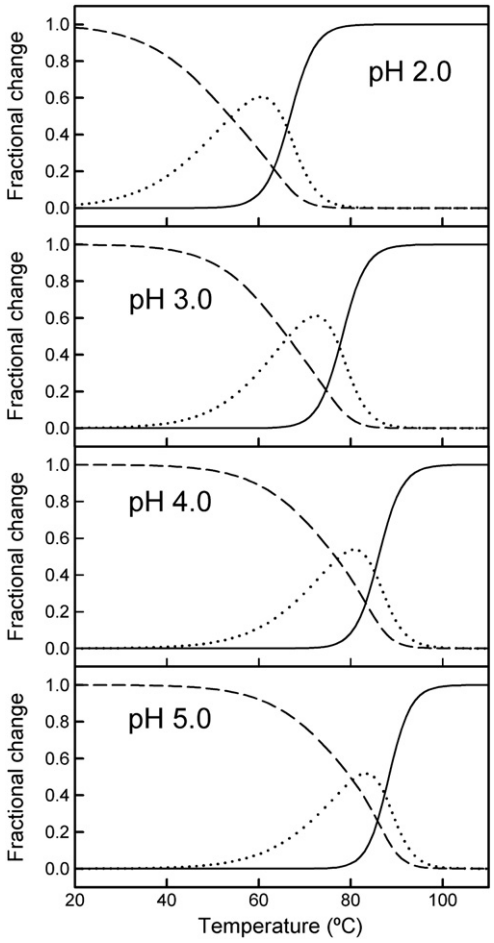

Fig. 6. Temperature dependence of the population of native (dashed lines), intermediate (dotted lines) and unfolded states (continuous lines), as calculated from the best fit of the three-state model.

Table 2
Thermodynamic parameters resulting from the best fit of the three-state sequential model, considering a native-like heat capacity for the intermediate, to the DSC traces.

pH	Tm^{N-I} (K)	ΔHm^{N-I} (kJ·mol^{-1})	Tm^{I-U} (K)	ΔHm^{I-D} (kJ·mol^{-1})	ΔC_p^{N-D} (kJ·K^{-1}·mol^{-1})
2.0	327.3 ± 1.2	112 ± 3	339.42 ± 0.08	333 ± 3	6.1 ± 0.3
3.0	339.1 ± 0.5	131.5 ± 1.5	350.74 ± 0.03	371.3 ± 1.6	5.4 ± 0.3
4.0	348.6 ± 1.6	142 ± 4	358.53 ± 0.13	395 ± 6	6.2 ± 0.4
5.0	350.3 ± 1.5	137 ± 4	360.76 ± 0.10	432 ± 5	5.4 ± 0.4
6.0	350.5 ± 2.0	148 ± 5	361.39 ± 0.14	437 ± 7	5.6 ± 0.5

Tm^{N-I} represents the temperature where the populations of native protein and intermediate are equal. At Tm^{I-U} the populations of intermediate species and unfolded protein are identical. ΔHm^{N-I} stands for the change in enthalpy at Tm^{N-I} and ΔHm^{N-I} for the change in enthalpy at Tm^{I-U}. ΔC_p^{N-U} is the global capacity change upon unfolding. Errors in ΔHm and Tm correspond to 3 times the fitting standard error. Errors in ΔC_p have been calculated by propagation.

In addition, onconase is not the only member of the ribonuclease A superfamily showing deviations from the two-state mechanism by thermal unfolding. For example, in the differential scanning calorimetry traces of the eosinophil cationic protein (ECP) there are two differentiated peaks [48]. Even ribonuclease A is known to unfold via an equilibrium intermediate, although this intermediate is a minor species (about 6% population) [49]. Other well known examples of ribonucleases of a similar size of onconase, albeit not from the ribonuclease A superfamily, not to unfold via a two-state mechanism are barnase [50] and ribonuclease H (at low pH values) [21].

Recently, we have studied the kinetics of onconase's folding process using guanidine as denaturant agent [51] and found an on-pathway kinetic folding intermediate. The data extrapolation to 0 M denaturant predicts that the energy barrier corresponding to the transition from the intermediate to the unfolded state is higher than the energy barrier of the native to intermediate transition. That would mean that the intermediate species should accumulate in the unfolding process in absence of denaturant agent and, therefore, it should be detected as an equilibrium intermediate. Clearly, our experimental data agree with these results.

It has also been reported that bovine pancreatic ribonuclease A, another member of the onconase superfamily (Fig. 7, panels A and B), associates in dimeric forms, after swapping of helix1, between two protein monomers (Fig. 7, panel C), under certain experimental

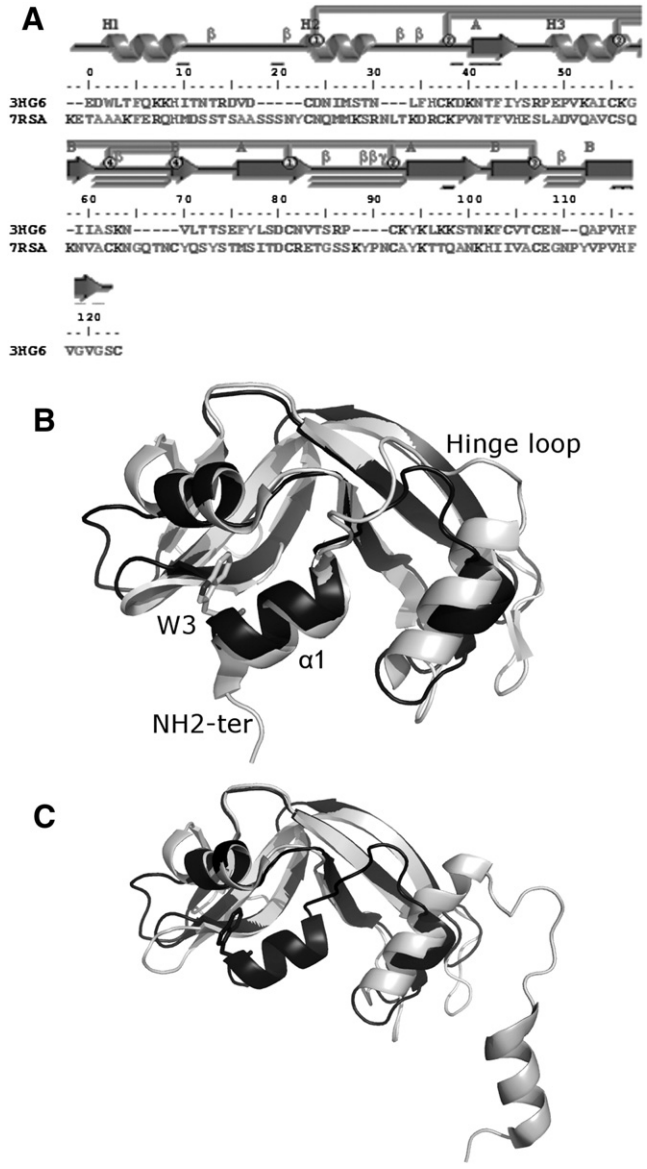

Fig. 7. Panel A: Amino acid sequence alignment of onconase and pancreatic ribonuclease A where a significantly shorter hinge loop for onconase can be appreciated. Panel B: comparison of the structures of onconase (dark grey) and ribonuclease A (light grey, PDB code 7rsa). Panel C: Comparison of onconase (dark grey) and ribonuclease A swapped structure (light grey, PDB code 1r5d) where the α1 helix is interchanged between monomers A and B to form an intertwined dimmer (for clarity, only chain A is shown).

conditions [52]. However, this does not seem to be the case for onconase's behaviour, since we do not see concentration dependence on thermal transitions. Also, helix1 swapping would be significantly more complicated for onconase, given that the hinge loop in onconase is shorter than that of ribonuclease A (Fig. 7, panels A and B). However, the "opening" of the hinge loop and subsequent detachment of helix1, which contains catalytic critical residues, could be a plausible explanation for our experimental results, as this movement would imply the exposure of hydrophobic patches, and the observed loss of Trp3 fluorescence. A better understanding of this folding intermediate and its biological implications requires a deeper study and thus, a detailed directed mutagenesis analysis of onconase is currently undergoing. Several single point mutations in different regions of the protein are currently being tested, especially focusing on the critical hinge loop and helix1 region.

4. Conclusions

The equilibrium thermal denaturation of onconase shows different denaturation temperatures depending on the spectroscopic probe that is being followed. Moreover, the DSC experiments are fully compatible with a three-state unfolding mechanism. Thus, the three-state sequential model can reproduce the experimental data very accurately. Therefore, the unfolding of onconase seems to take place through, at least, one equilibrium intermediate, whose stability is close to the stability of the native protein and that implies the loss of about 25% of the interaction energy and some structural changes around Trp3.

Acknowledgements

The authors would like to thank Alfacell Corp. for the gift of the plasmid to express onconase, Prof. Franz X. Schmid (Universität Bayreuth) for the use of the CD-spectrometer, VP-calorimeter and helpful discussions, and Cindy Schulenburg (Martin-Luther-Universität Halle-Wittenberg) for fruitful discussions and onconase samples to compare. We wish to thank the Laboratory of Crystallographic Studies (LEC), for the crystallization and x-ray diffraction data collection, as well as the staff at BM16 (ESRF), for their assistance during data collection.

S.C.-A. is recipient of a Juan de la Cierva postdoctoral research contract from the Spanish Ministry of Science.

This research was funded by a Grant CVI-02806 from the Andalusian Government, and the "Factoría Española de cristalización" Consolider-Ingenio 2010 project, from the Spanish Ministry of Science.

Appendix A. Supplementary data

Supplementary data to this article can be found online at doi:10.1016/j.bpc.2011.07.005.

References

[1] Z. Darzynkiewicz, S.P. Carter, S.M. Mikulski, W.J. Ardelt, K. Shogen, Cytostatic and cytotoxic effects of Pannon (P-30 Protein), a novel anticancer agent, Cell Tissue Kinet 21 (1988) 169–182.
[2] S.M. Mikulski, W. Ardelt, K. Shogen, E.H. Bernstein, H. Menduke, Striking increase of survival of mice bearing M109 Madison carcinoma treated with a novel protein from amphibian embryos, J. Natl. Cancer Inst. 82 (1990) 151–153.
[3] I. Lee, Y.H. Lee, S.M. Mikulski, K. Shogen, Effect of ONCONASE +/− tamoxifen on ASPC-1 human pancreatic tumors in nude mice, Adv. Exp. Med. Biol. 530 (2003) 187–196.
[4] M. Michaelis, J. Cinatl, P. Anand, F. Rothweiler, R. Kotchetkov, A. Deimling, H.W. Doerr, K. Shogen, J. Cinatl Jr., Onconase induces caspase-independent cell death in chemoresistant neuroblastoma cells, Cancer Lett. 250 (2007) 107–116.
[5] W. Ardelt, K. Shogen, Z. Darzynkiewicz, Onconase and amphinase, the antitumor ribonucleases from Rana pipiens oocytes, Curr. Pharm. Biotechnol. 9 (2008) 215–225.
[6] S.K. Saxena, R. Sirdeshmukh, W. Ardelt, S.M. Mikulski, K. Shogen, R.J. Youle, Entry into cells and selective degradation of tRNAs by a cytotoxic member of the RNase A family, J. Biol. Chem. 277 (2002) 15142–15146.
[7] S.K. Saxena, M. Gravell, Y.N. Wu, S.M. Mikulski, K. Shogen, W. Ardelt, R.J. Youle, Inhibition of HIV-1 production and selective degradation of viral RNA by an amphibian ribonuclease, J. Biol. Chem. 271 (1996) 20783–20788.
[8] R.J. Youle, Y.N. Wu, S.M. Mikulski, K. Shogen, R.S. Hamilton, D. Newton, G. D'Alessio, M. Gravell, RNase inhibition of human immunodeficiency virus infection of H9 cells, Proc. Natl. Acad. Sci. U. S. A. 91 (1994) 6012–6016.
[9] V.M. Vasandani, Y.N. Wu, S.M. Mikulski, R.J. Youle, C. Sung, Molecular determinants in the plasma clearance and tissue distribution of ribonucleases of the ribonuclease A superfamily, Cancer Res. 56 (1996) 4180–4186.
[10] V.M. Vasandani, J.A. Burris, C. Sung, Reversible nephrotoxicity of onconase and effect of lysine pH on renal onconase uptake, Cancer Chemother. Pharmacol. 44 (1999) 164–169.
[11] E. Notomista, F. Catanzano, G. Graziano, F. Dal Piaz, G. Barone, G. D'Alessio, A. Di Donato, Onconase: an unusually stable protein, Biochemistry 39 (2000) 8711–8718.
[12] C.A. Royer, The nature of the transition state ensemble and the mechanisms of protein, Arch. Biochem. Biophys. 469 (2008) 34–45.
[13] R. Melki, N.J. Cowan, Facilitated folding of actins and tubulins occurs via a nucleotide-dependent interaction between cytoplasmic chaperonin and distinctive folding intermediates, Mol. Cell. Biol. 14 (1994) 2895–2904.

[14] F. Chiti, C.M. Dobson, Protein misfolding, functional amyloid, and human disease, Annu. Rev. Biochem. 75 (2006) 333–366.
[15] A.C. Ferreon, A.A. Deniz, Alpha-synuclein multistate folding thermodynamics: implications for protein misfolding and aggregation, Biochemistry 46 (2007) 4499–4509.
[16] A.C. Apetri, K. Maki, H. Roder, W.K. Surewicz, Early intermediate in human prion protein folding as evidenced by ultrarapid mixing experiments, J. Am. Chem. Soc. 128 (2006) 11673–11678.
[17] L.A. Campos, M.M. Garcia-Mira, R. Godoy-Ruiz, J.M. Sanchez-Ruiz, J. Sancho, Do proteins always benefit from a stability increase? Relevant and residual stabilisation in a three-state protein by charge optimisation, J. Mol. Biol. 344 (2004) 223–237.
[18] M.P. Irun, M.M. Garcia-Mira, J.M. Sanchez-Ruiz, J. Sancho, Native hydrogen bonds in a molten globule: the apoflavodoxin thermal intermediate, J. Mol. Biol. 306 (2001) 877–888.
[19] E.S. Cobos, M. Iglesias-Bexiga, J. Ruiz-Sanz, P.L. Mateo, I. Luque, J.C. Martinez, Thermodynamic characterization of the folding equilibrium of the human Nedd4-WW4 domain: at the frontiers of cooperative folding, Biochemistry 48 (2009) 8712–8720.
[20] Y. Luo, M.S. Kay, R.L. Baldwin, Cooperativity of folding of the apomyoglobin pH 4 intermediate studied by glycine and proline mutations, Nat. Struct. Biol. 4 (1997) 925–930.
[21] J.M. Dabora, S. Marqusee, Equilibrium unfolding of Escherichia coli ribonuclease H: characterization of a partially folded state, Protein Sci. 3 (1994) 1401–1408.
[22] U. Arnold, C. Schulenburg, D. Schmidt, R. Ulbrich-Hofmann, Contribution of structural peculiarities of onconase to its high stability and folding kinetics, Biochemistry 45 (2006) 3580–3587.
[23] A. Camara-Artigas, A. Palencia, J.C. Martinez, I. Luque, J.A. Gavira, J.M. Garcia-Ruiz, Crystallization by capillary counter-diffusion and structure determination of the N114A mutant of the SH3 domain of Abl tyrosine kinase complexed with a high-affinity peptide ligand, Acta Crystallogr. D Biol. Crystallogr. 63 (2007) 646–652.
[24] Z. Otwinowski, W. Minor, Processing of X-ray diffraction data collected in oscillation mode, in: J. Charles, W. Carter (Eds.), Methods in Enzymology, Macromolecular Crystallography, Part A, Academic Press, 1997, pp. 307–326.
[25] A. Vagin, A. Teplyakov, MOLREP: an automated program for molecular replacement, J. Appl. Crystallogr. 30 (1997) 1022–1025.
[26] B.W. Matthews, Solvent content of protein crystals, J. Mol. Biol. 33 (1968) 491–497.
[27] P. Emsley, K. Cowtan, Coot: model-building tools for molecular graphics, Acta Crystallogr. D Biol. Crystallogr. 60 (2004) 2126–2132.
[28] S. Bailey, The CCP4 suite: programs for protein crystallography, Acta Crystallogr. D Biol. Crystallogr. 50 (1994) 760–763.
[29] S.C. Lovell, I.W. Davis, W.B. Arendall III, P.I. de Bakker, J.M. Word, M.G. Prisant, J.S. Richardson, D.C. Richardson, Structure validation by Calpha geometry: phi, psi and Cbeta deviation, Proteins 50 (2003) 437–450.
[30] R.A. Laskowski, M.W. MacArthur, D.S. Moss, J.M. Thornton, PROCHECK: a program to check the stereochemical quality of protein structures, J. Appl. Crystallogr. 26 (1993) 283–291.
[31] C. Schulenburg, M.M. Martinez-Senac, C. Low, R. Golbik, R. Ulbrich-Hofmann, U. Arnold, Identification of three phases in Onconase refolding, FEBS J. 274 (2007) 5826–5833.
[32] R.E. Georgescu, M.M. Garcia-Mira, M.L. Tasayco, J.M. Sanchez-Ruiz, Heat capacity analysis of oxidized Escherichia coli thioredoxin fragments (1–73, 74–108) and their noncovalent complex. Evidence for the burial of apolar surface in protein unfolded states, Eur. J. Biochem. 268 (2001) 1477–1485.
[33] E. Freire, Differential scanning calorimetry, in: B.A. Shirley (Ed.), Protein Stability and Folding: Theory and Practice, Humana Press, Totowa, New Jersey, 1995, pp. 191–218.
[34] P.L. Privalov, G.I. Makhatadze, Heat capacity of proteins. II. Partial molar heat capacity of the unfolded polypeptide chain of proteins: protein unfolding effects, J. Mol. Biol. 213 (1990) 385–391.
[35] J.C. Martinez, A.R. Viguera, R. Berisio, M. Wilmanns, P.L. Mateo, V.V. Filimonov, L. Serrano, Thermodynamic analysis of alpha-spectrin SH3 and two of its circular permutants with different loop lengths: discerning the reasons for rapid folding in proteins, Biochemistry 38 (1999) 549–559.
[36] A.M. Candel, N.A. van Nuland, F.M. Martin-Sierra, J.C. Martinez, F. Conejero-Lara, Analysis of the thermodynamics of binding of an SH3 domain to proline-rich peptides using a chimeric fusion protein, J. Mol. Biol. 377 (2008) 117–135.
[37] P.R. Bevington, D.K. Robinson, Data Reduction and Error Analysis for the Physical Sciences, McGraw-Hill, New York, 2003.
[38] E.S. Cobos, A.M. Candel, J.C. Martinez, An error analysis for two-state protein-folding kinetic parameters and phi-values: progress toward precision by exploring pH dependencies on Leffler plots, Biophys. J. 94 (2008) 4393–4404.
[39] C. Schulenburg, U. Weininger, P. Neumann, H. Meiselbach, M.T. Stubbs, H. Sticht, J. Balbach, R. Ulbrich-Hofmann, U. Arnold, Impact of the C-terminal disulfide bond on the folding and stability of onconase, ChemBioChem 11 (2010) 978–986.
[40] P.L. Privalov, E.I. Tiktopulo, S. Venyaminov, V. Griko Yu, G.I. Makhatadze, N.N. Khechinashvili, Heat capacity and conformation of proteins in the denatured state, J. Mol. Biol. 205 (1989) 737–750.
[41] B. Beermann, J. Guddorf, K. Boehm, A. Albers, S. Kolkenbrock, S. Fetzner, H.J. Hinz, Stability, unfolding, and structural changes of cofactor-free 1H-3-hydroxy-4-oxoquinaldine 2,4-dioxygenase, Biochemistry 46 (2007) 4241–4249.
[42] T. Derrick, A.O. Grillo, S.N. Vitharana, L. Jones, J. Rexroad, A. Shah, M. Perkins, T.M. Spitznagel, C.R. Middaugh, Effect of polyanions on the structure and stability of repifermin (keratinocyte growth factor-2), J. Pharm. Sci. 96 (2007) 761–776.
[43] M.R. Eftink, C.A. Ghiron, Fluorescence quenching studies with proteins, Anal. Biochem. 114 (1981) 199–227.
[44] M. Hameed, B. Ahmad, K.M. Fazili, K. Andrabi, R.H. Khan, Different molten globule-like folding intermediates of hen egg white lysozyme induced by high pH and tertiary butanol, J. Biochem. 141 (2007) 573–583.
[45] T. Kiefhaber, F.X. Schmid, K. Willaert, Y. Engelborghs, A. Chaffotte, Structure of a rapidly formed intermediate in ribonuclease T1 folding, Protein Sci. 1 (1992) 1162–1172.
[46] J.H. Kleinschmidt, L.K. Tamm, Time-resolved distance determination by tryptophan fluorescence quenching: probing intermediates in membrane protein folding, Biochemistry 38 (1999) 4996–5005.
[47] L.A. Campos, M. Bueno, J. Lopez-Llano, M.A. Jimenez, J. Sancho, Structure of stable protein folding intermediates by equilibrium phi-analysis: the apoflavodoxin thermal intermediate, J. Mol. Biol. 344 (2004) 239–255.
[48] Z. Nikolovski, V. Buzon, M. Ribo, M. Moussaoui, M. Vilanova, C.M. Cuchillo, J. Cladera, M.V. Nogues, Thermal unfolding of eosinophil cationic protein/ribonuclease 3: a nonreversible process, Protein Sci. 15 (2006) 2816–2827.
[49] R.L. Baldwin, The search for folding intermediates and the mechanism of protein folding, Annu. Rev. Biophys. 37 (2008) 1–21.
[50] P.A. Dalby, M. Oliveberg, A.R. Fersht, Folding intermediates of wild-type and mutants of barnase. I. Use of phi-value analysis and m-values to probe the cooperative nature of the folding pre-equilibrium, J. Mol. Biol. 276 (1998) 625–646.
[51] C. Schulenburg, C. Low, U. Weininger, C. Mrestani-Klaus, H. Hofmann, J. Balbach, R. Ulbrich-Hofmann, U. Arnold, The folding pathway of onconase is directed by a conserved intermediate, Biochemistry 48 (2009) 8449–8457.
[52] E. Bucci, L. Vitagliano, R. Barone, S. Sorrentino, G. D'Alessio, G. Graziano, On the thermal stability of the two dimeric forms of ribonuclease A, Biophys. Chem. 116 (2005) 89–95.